Chemical Science

ROYAL SOCIETY OF CHEMISTRY

EDGE ARTICLE

View Article Online
View Journal | View Issue

Cite this: *Chem. Sci.*, 2025, **16**, 16070

All publication charges for this article have been paid for by the Royal Society of Chemistry

A pair of strongly reductive and oxidative photocatalysts for the general upcycling of biomass derivatives and plastic wastes†

Hao Cui,‡ Xiang Chen,‡ Xiong She, Wen-Xin Su, Shi-Chao Chen and Xiao Zhang *

Tailoring photocatalysts to achieve both strongly reductive and oxidative properties from a common scaffold remains challenging. Herein, we report the development of a pair of photocatalysts, isothiatruxene (ITS) and isosulfonyltruxene ($ITSO_2$), by modulating the valence states of heteroatoms. ITS exhibits highly reducing power, facilitating selective cleavage of C–O bonds in biomass derivatives despite their negative redox potentials. Upon oxidation of ITS, the resultant $ITSO_2$ demonstrates strongly oxidizing capacity, enabling metal-free and acid-free upcycling of plastic wastes even with their high redox potentials. By immobilizing ITS and $ITSO_2$ on polystyrene and oxidized lignin supports, respectively, we have developed recyclable photocatalysts that drive multiple catalytic cycles with high efficiency. Gram-scale upcycling of plastic is achieved by integrating photoredox catalysis with flow chemistry. Mechanistic studies reveal that the excited states of ITS and $ITSO_2$ can directly activate inert substrates, correlating with their strong redox properties. The newly introduced pair of photocatalysts, characterized by their metal-free nature, concise synthesis *via* trimerization, and dual photocatalytic capabilities encompassing both strongly reducing and oxidizing properties, show great potential for a wide range of applications. Furthermore, this study presents a sustainable catalytic strategy for synthesizing high-value aromatic compounds directly from biomass derivatives and plastic wastes.

Received 13th May 2025
Accepted 21st July 2025

DOI: 10.1039/d5sc03457d

rsc.li/chemical-science

Introduction

Photoredox catalysis has emerged as a powerful tool for enabling previously challenging transformations through the selective activation of compounds *via* radical processes.[1–11] Central to this approach are photocatalysts (PCs), which, upon irradiation, attain short-lived yet highly reactive excited states that mediate subsequent single-electron transfer (SET) events. The development of PCs with highly reducing[12–34] or oxidizing[35–41] capacities is of particular significance due to their ability to activate inert substrates. However, modulating PCs to simultaneously achieve both high reduction and oxidation potentials from a common scaffold is challenging. In this regard, altering the ligands around the metal center represents a flexible strategy to tune the redox properties.[42] For instance, modifying electron-donating ligands [*e.g.*, *fac*-Ir(ppy)$_3$: $E_{1/2}(PC^{\bullet+}/PC^*) = -1.73$ V *vs.* SCE] or electron-withdrawing ligands {*e.g.*, Ir[dF(CF$_3$)ppy]$_2$(dtbbpy)PF$_6$: $E_{1/2}(PC^*/PC^{\bullet-}) = +1.21$ V *vs.* SCE} around iridium complexes can access ambivalent reducing and oxidizing capacities (Fig. 1A). Alternatively, the photophysical properties of organic PCs can be readily tuned by altering the donor or acceptor substituents around their structural cores.[43] For example, systematic modifications of 1,2,3,5-tetrakis(carbazol-9-yl)-4,6-dicyanobenzene (4CzIPN) have identified that the excited-state redox potentials for the strongly reducing 3DPA2FBN and the potent oxidizing 3CzClIPN are −1.60 V and + 1.56 V (*vs.* SCE), respectively (Fig. 1B). Despite these advances, the development of PCs that can simultaneously achieve even stronger reducing and oxidizing capacities for activating more inert substrates remains underexplored.

The over-reliance on non-renewable fossil fuels has led to rapid resource depletion and significant environmental issues. Meanwhile, the large-scale accumulation of plastic wastes in landfills and ecosystems has caused severe environmental, safety, and health problems, as well as substantial resource waste. Therefore, the development of approaches for the sustainable utilization of renewable biomass[44–49] and plastic wastes[50–67] has become a critical priority to address these alarming dilemmas. However, the inert chemical bonds within biomass and plastics pose significant challenges for their upcycling into value-added chemicals. For instance, lignin, a key biomass component, contains multiple interunit linkages, with the β-O-4 bond (BDE = 274 kJ mol^{-1}) being predominant

Fujian Key Laboratory of Polymer Materials, Fujian Provincial Key Laboratory of Advanced Materials Oriented Chemical Engineering, College of Chemistry and Materials Science, Fujian Normal University, Fuzhou 350117, China. E-mail: zhangxiao@fjnu.edu.cn

† Electronic supplementary information (ESI) available: Experimental and copies of NMR spectra. CCDC 2412529 and 2412532. For ESI and crystallographic data in CIF or other electronic format see DOI: https://doi.org/10.1039/d5sc03457d

‡ These authors contributed equally to this work.

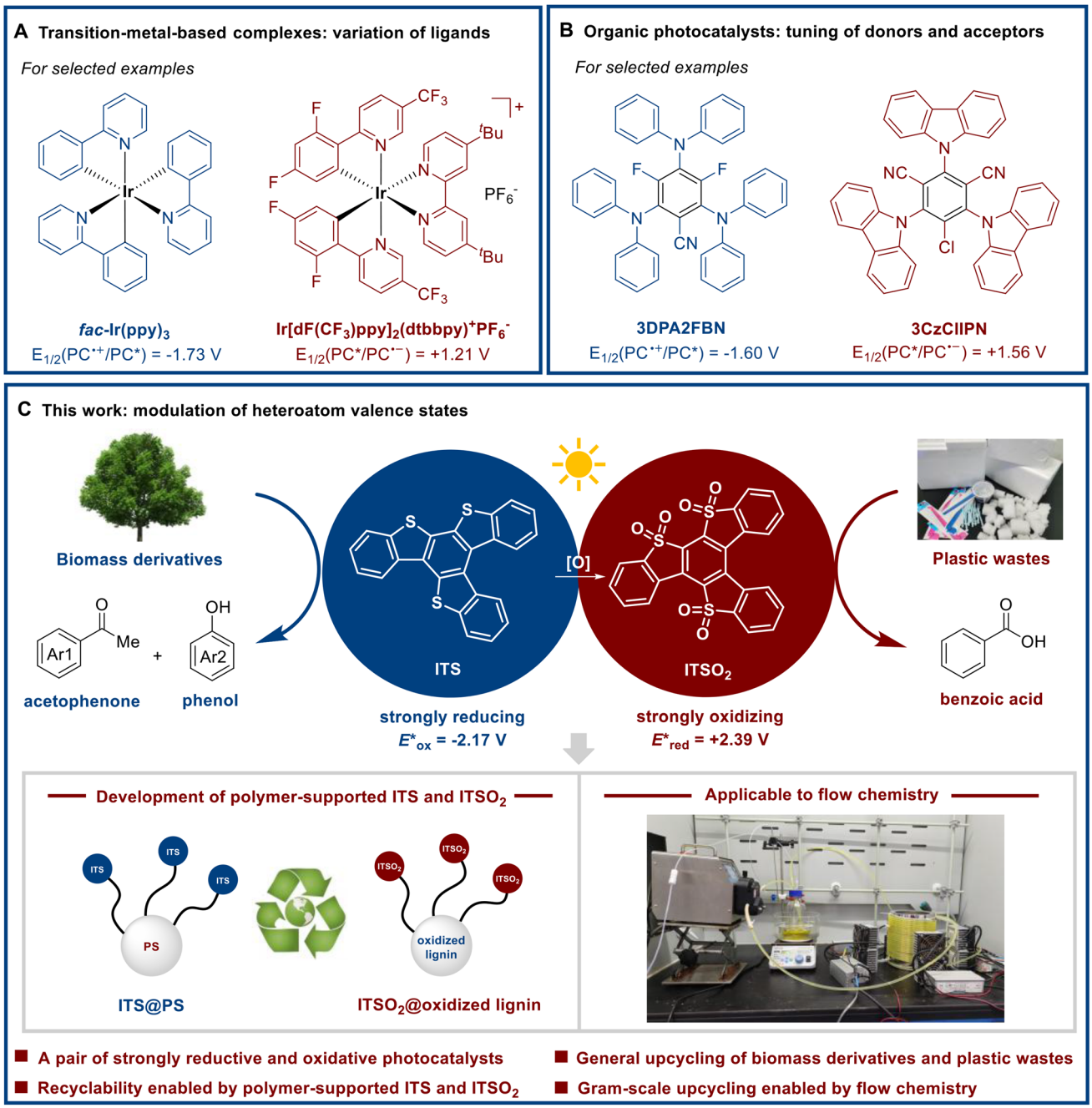

Fig. 1 Strategies for tailoring photocatalysts to achieve both strongly reductive and oxidative properties (potentials are given *versus* the saturated calomel electrode (SCE)).

in both softwood and hardwood varieties.[68] Traditional methods for lignin depolymerization suffer from stringent conditions and intensive energy input. Similarly, polystyrene (PS), a major plastic, is resistant to degradation due to its strong C–C bonds (BDE = 356 kJ mol^{-1}).[69] Conventional thermochemical treatment processes often require precious metal catalysts and harsh reaction conditions, such as high pressure or elevated temperature. Recently, photocatalysis has emerged as an attractive and effective tool to convert PS into small valuable molecules. However, most photocatalytic upcycling methods employ metal-based catalysts or acid additives to facilitate the degradation process. Therefore, the development of metal-free and environmentally friendly strategies for the upcycling of biomass derivatives[70,71] and plastic wastes[72–88] is highly desirable.

Herein, we introduce a pair of highly reductive and oxidative photocatalysts, isothiatruxene (**ITS**) and isosulfonyltruxene (**$ITSO_2$**), which are derived from the same starting materials through modulation of heteroatom valence states (Fig. 1C). Isothiatruxene (**ITS**) is readily synthesized *via* direct

trimerization of benzothiophene, and a single-step oxidation with *m*-CPBA converts it to isosulfonyltruxene (**ITSO$_2$**).[89–91] Photophysical characterization reveals that **ITS** possesses strong reducing power ($E^*_{1/2} = -2.17$ V *vs.* SCE), whereas **ITSO$_2$** exhibits significant oxidizing ability ($E^*_{1/2} = +2.39$ V *vs.* SCE). Notably, the combined redox potential window of **ITS** and **ITSO$_2$** exceeds that of conventional photocatalysts. To address the challenges in upcycling biomass derivatives and plastic wastes, we explored whether the combination of **ITS** and **ITSO$_2$** could provide a general strategy for cleaving inert bonds in these materials under mild visible-light conditions. This approach would enable the direct synthesis of valuable aromatic building blocks, such as acetophenone, phenol, and benzoic acid, from biomass derivatives and plastic wastes. It was found that **ITS** photocatalysis can efficiently cleave C–O bonds in oxidized lignin models, vanillin-derived crosslinked polymer, and native oxidized lignin at room temperature under reductive conditions, despite the highly negative redox potentials of ketone moieties [*e.g.*, $E_{1/2} = -2.11$ V *vs.* SCE for acetophenone].[92] Similarly, **ITSO$_2$** photocatalysis converts polystyrene and real-world plastics into benzoic acid under oxidative conditions, even with the high redox potentials of arene groups [*e.g.*, $E_{1/2} = +2.36$ V *vs.* SCE for toluene].[92] The recyclability of catalysts is achieved by introducing polystyrene-supported **ITS** and oxidized lignin-supported **ITSO$_2$**, thereby enhancing the practicality. Importantly, this protocol is amenable to continuous flow processing, facilitating gram-scale upcycling under ambient conditions. Mechanistic studies correlate with the strongly reducing and oxidizing properties of this pair of PCs, in which inert substrates can be directly activated by their excited states.

Results and discussion

Both isothiatruxene (**ITS**) and isosulfonyltruxene (**ITSO$_2$**) were rapidly synthesized from the same starting material. While **ITS** was prepared through 2,3-dichloro-5,6-dicyano-1,4-benzoquinone (DDQ)-enabled trimerization of benzothiophene, subsequent oxidation of **ITS** with *meta*-chloroperoxybenzoic acid (*m*-CPBA) afforded **ITSO$_2$** in a single step (Fig. 2A).[93] X-ray crystallographic analysis further confirmed the heteroatom valence states in **ITSO$_2$**.[93] The UV/vis absorption spectrum of **ITS** exhibits a maximum at 389 nm, with a tailed absorption edge extending into the visible region. Comparatively, **ITSO$_2$** shows enhanced visible-light absorption with a notable bathochromic shift (Fig. 2B). The emission maximum of **ITSO$_2$** was consistently more red-shifted than that of **ITS** (Fig. 2C). The intersection points of the normalized absorbance and emission spectra were determined to be 394 nm for **ITS** and 405 nm for **ITSO$_2$**, corresponding to zero–zero vibrational state excitation energies ($E_{0,0}$) of 3.15 eV and 3.06 eV, respectively (Fig. S4 and S12 in the ESI†). Cyclic voltammetry measurements provided the ground-state potentials ($E_{1/2}$) of **ITS** and **ITSO$_2$** (Fig. S5–S8 and S13–S15 in the ESI†). Based on these potentials and the $E_{0,0}$ values, the excited-state oxidation potential of **ITS** and the excited-state reduction potential of **ITSO$_2$** were calculated to be −2.17 V and +2.39 V, respectively.[93] The fluorescence lifetime decay curves revealed excited-state lifetimes of 1.23 ns for **ITS** and 1.70 ns for **ITSO$_2$** (Fig. 2D). Collectively, these results demonstrate that this pair of photocatalysts exhibits both strongly reducing and oxidizing capacities through the simple tuning of heteroatom valence states.

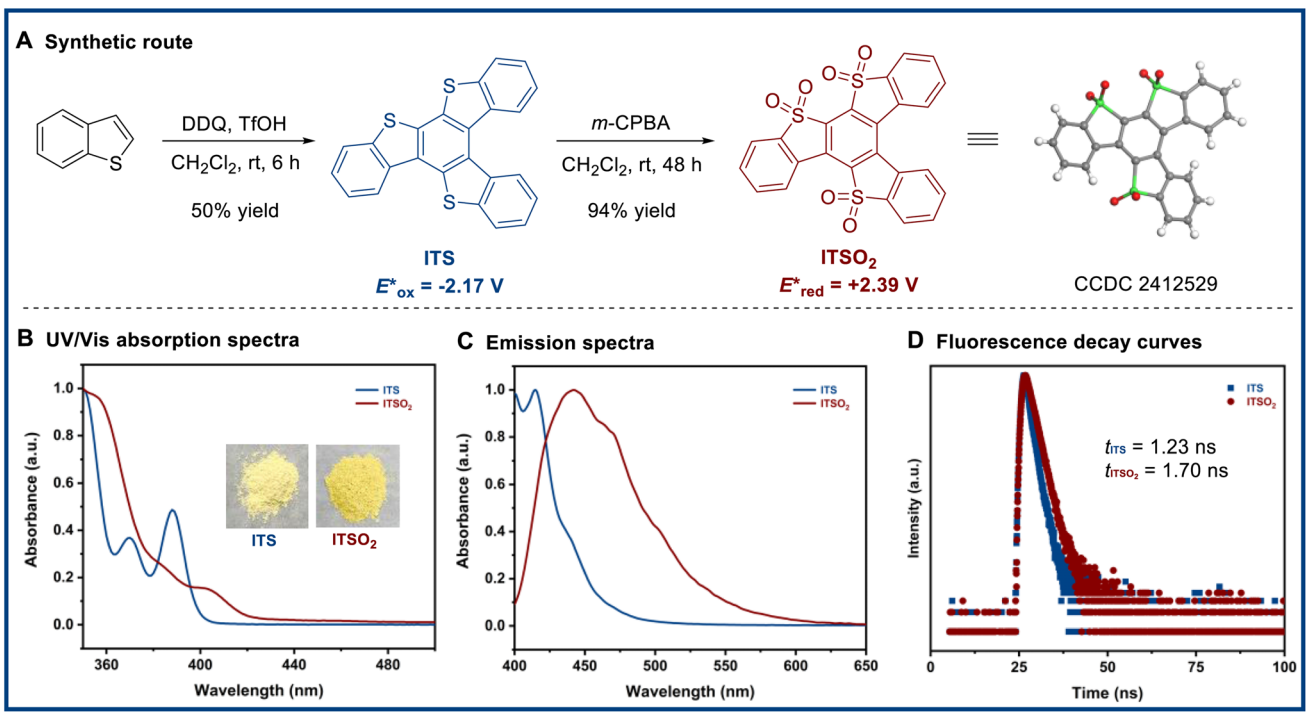

Fig. 2 Development of a pair of strongly reductive and oxidative photocatalysts: ITS and $ITSO_2$.

Owing to the strongly reducing ability of **ITS**, its capacity to cleave oxidized β-O-4 lignin models was investigated (left column, Fig. 3A). With DIPEA and HCOOH as additives, the reductive C–O bond cleavage of model substrate (**1a**) proceeded smoothly in toluene under blue LED irradiation, affording the expected products *p*-methoxyacetophenone (**2a**) and 4-biphenylol (**3a**) in 89% yield and 90% yield, respectively (entry 1). Notably, the choice of solvent significantly influenced the outcome. While dichloromethane provided comparable results, inferior yields of **2a** and **3a** were achieved in the presence of methanol (entries 2 and 3). When the solvent was changed to dimethyl sulfoxide, acetonitrile, acetone, or ethyl acetate, the *p*-

A Photocatalytic cleavage of oxidized ß-O-4 lignin models

Optimization of the reaction conditions

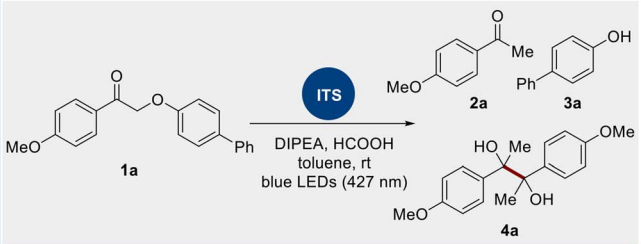

Entry	Variations from standard conditions[a]	Yield (%)[b] 2a	3a	4a
1	none	92 (89)[c]	94 (90)[c]	
2	CH_2Cl_2 instead of toluene	90	88	
3	MeOH instead of toluene	40	46	
4	DMSO instead of toluene		92	88
5	CH_3CN instead of toluene		94	91
6	acetone instead of toluene		91	89
7	EtOAc instead of toluene		90	88
8	no HCOOH	80	82	
9	no DIPEA	88	53	
10	no ITS	5	5	
11	no light		N.R.	

[a]Reaction conditions: a solution of **ITS** (2.0 mg, 5.0 mol%), **1a** (0.1 mmol), DIPEA (0.3 mmol), and HCOOH (0.3 mmol) in toluene (1.0 mL) was irradiated by 427 nm Kessil lamp (40 W) at room temperature under nitrogen atmosphere for 20 h.
[b]Determined by ^{1}H NMR yield using CH_2Br_2 as an internal standard.
[c]Isolated yield.
DIPEA = *N*,*N*-diisopropylethylamine. N.R. = no reaction

Substrate Scope

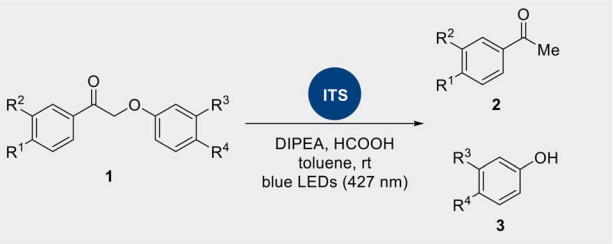

Entry	Substrates (1)[a]	Yield (%)[b] Acetophenones (2)	Phenols (3)
1	R^1 = OMe, R^2,R^3 = H, R^4 = Ph (**1a**)	89 (**2a**)	89 (**3a**)
2	R^1 = OMe, R^2,R^3 = H, R^4 = Cl (**1b**)	90 (**2a**)	91 (**3b**)
3	R^1 = OMe, R^2,R^3 = H, R^4 = ^{t}Bu (**1c**)	81 (**2a**)	88 (**3c**)
4	R^1 = OMe, R^2,R^3 = H, R^4 = OMe (**1d**)	83 (**2a**)	87 (**3d**)
5	R^1 = OMe, R^2 = H, R^3,R^4 = -CH=CH-CH=CH- (**1e**)	90 (**2a**)	88 (**3e**)
6	R^1,R^2 = OMe, R^3,R^4 = H (**1f**)	84 (**2b**)	94 (**3f**)
7	R^1,R^2 = OMe, R^3 = H, R^4 = Ph (**1g**)	87 (**2b**)	95 (**3a**)
8	R^1,R^2 = OMe, R^3 = H, R^4 = OMe (**1h**)	86 (**2b**)	96 (**3d**)
9	R^1 = Cl, R^2,R^3 = H, R^4 = Ph (**1i**)	85 (**2c**)	90 (**3a**)
10	R^1,R^2,R^3,R^4 = H (**1j**)	95 (**2d**)	91 (**3f**)
11	R^1 = Ph, R^2,R^3,R^4 = H (**1k**)	89 (**2e**)	87 (**3f**)
12	R^1,R^2 = -CH=CH-CH=CH-, R^3,R^4 = H (**1l**)	90 (**2f**)	88 (**3f**)

[a]Reaction conditions: a solution of **ITS** (4.0 mg, 5.0 mol%), **1** (0.2 mmol), DIPEA (0.6 mmol), and HCOOH (0.6 mmol) in toluene (2.0 mL) was irradiated by 427 nm Kessil lamp (40 W) at room temperature under nitrogen atmosphere for 10-21 h.
[b]Isolated yield.

B Photocatalytic degradation of biomass-derived crosslinked polymer

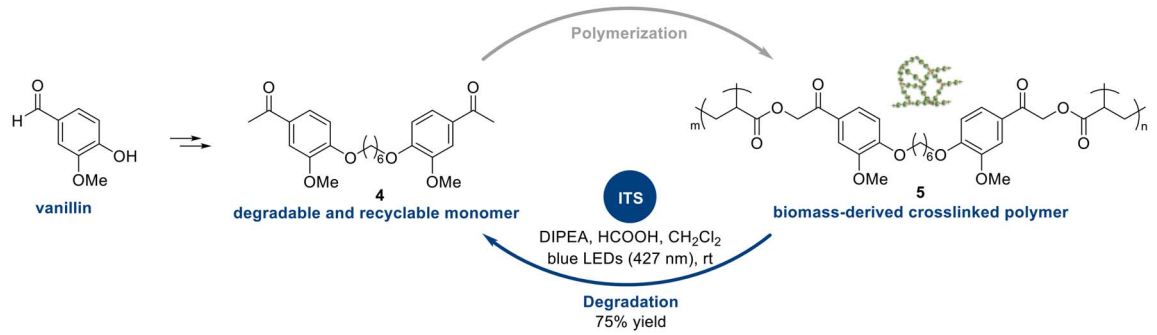

C Photocatalytic upcycling of native oxidized lignin

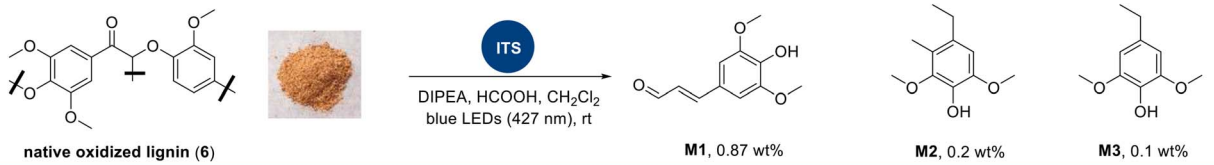

Fig. 3 Photocatalytic upcycling of biomass derivatives enabled by ITS.

methoxyacetophenone (**2a**) product underwent a secondary pinacol-type coupling, resulting in the formation of 1,2-diol **4a** instead (entries 4–7). The absence of either HCOOH or DIPEA led to slightly decreased yields of **2a** and **3a** (entries 8 and 9). Control experiments further demonstrated that both **ITS** and visible light are essential for this transformation (entries 10 and 11).

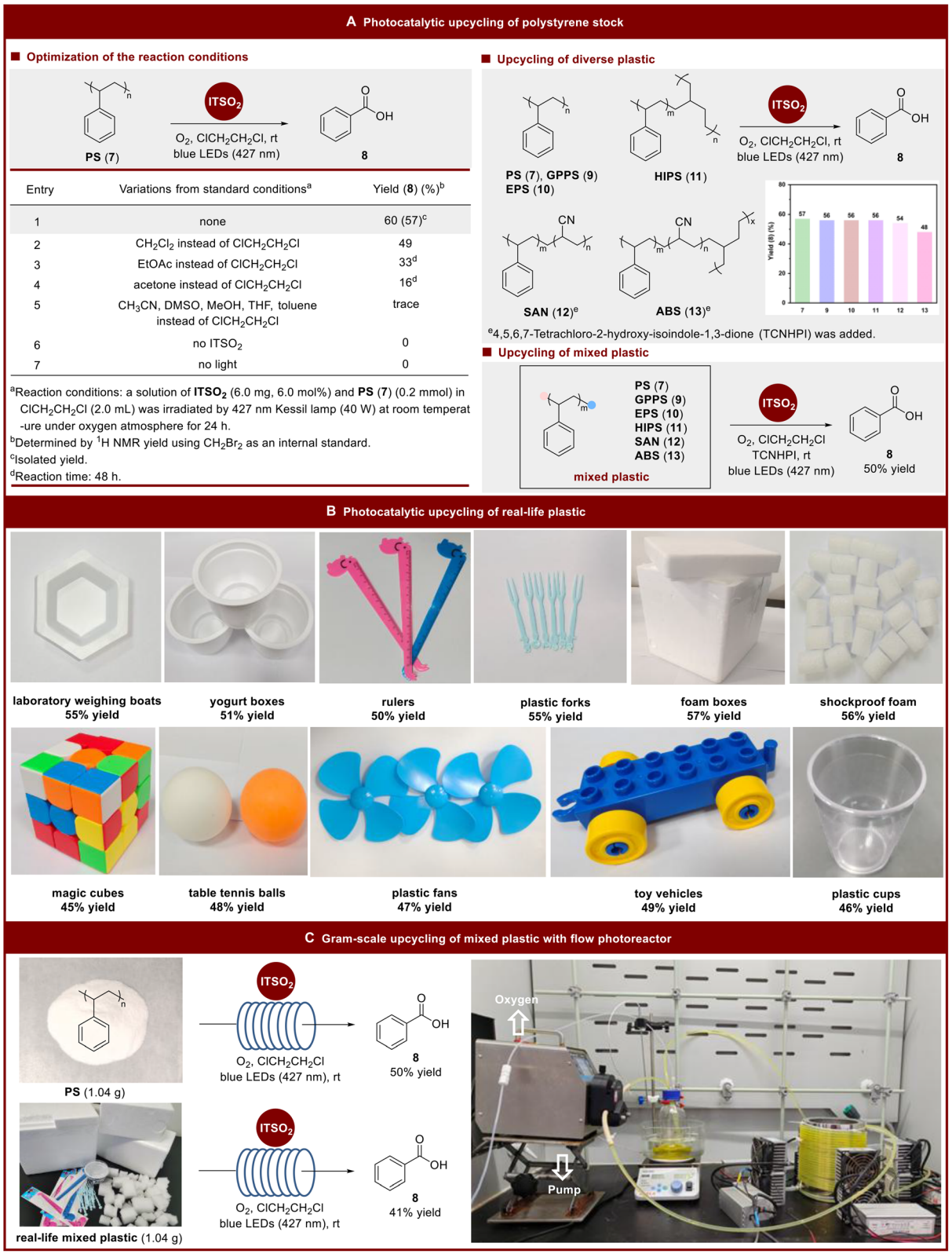

Fig. 4 Photocatalytic upcycling of plastic wastes enabled by $ITSO_2$.

Under the optimized reaction conditions, the scope of β-O-4 ketones was evaluated (right column, Fig. 3A). When oxidized β-O-4 lignin models bearing diverse substituents (–Ph, –Cl, –^{t}Bu, –OMe) at the *para*-position of the phenol moieties were tested under the photocatalysis of **ITS**, selective C–O bond cleavage was uniformly achieved, delivering *p*-methoxyacetophenone (**2a**) and functionalized phenols (**3a–d**) in good yields (entries 1–4). Similarly, a naphthalene-derived substrate **1e** underwent efficient C–O bond cleavage, affording *p*-methoxyacetophenone (**2a**) and naphthalen-2-ol (**3e**) in 90% and 88% yields, respectively (entry 5). This method is also applicable to substrates (**1f–h**) bearing di-electron-donating MeO– groups on the aromatic ketones, despite their more negative redox potentials (entries 6–8). Substrates **1i–l** were tolerated, leading to the corresponding acetophenones and phenols with high efficiency (entries 9–12).

The catalytic utility of **ITS** was subsequently probed in the degradation of biomass-derived crosslinked polymer (Fig. 3B). As an elegant precedence, biomass-derived crosslinked polymer **5**, which was designed and synthesized from vanillin, can be programmed at ~300 nm to degrade with ~60% recovery of the monomer **4**.[94] This method mainly relied on the excited state reactivity of ketone moieties under ultraviolet light. In a complementary fashion, we envisioned that **ITS** catalysis may provide a catalytic and mechanistically distinct single-electron-transfer (SET) approach by directly harnessing abundant visible light. To our delight, by utilizing **ITS** as the photocatalyst, DIPEA as the stoichiometric reductant in concert with formic acid, and dichloromethane as the solvent, the desired C–O cleavage product **4** was obtained in 75% yield under irradiation with blue LEDs (Fig. 3B). As such, this method offers a complementary sustainable strategy to address the issue of degradability.

Encouraged by these results, we sought to explore the potential of **ITS** to catalyze the depolymerization of native oxidized lignin (**6**), which is particularly challenging due to its highly robust and complex structure (Fig. 3C). Irradiating a reaction mixture containing 20.0 mg of oxidized lignin, 2.0 mg of **ITS** photocatalyst, and DIPEA/HCOOH additives in dichloromethane with blue LEDs for 48 hours resulted in an organic-soluble fraction, along with an insoluble solid fraction. Gratifyingly, gas chromatography-mass spectrometry (GC-MS) analysis of the soluble fraction identified at least three monomeric products: 3-(4-hydroxy-3,5-dimethoxyphenyl) acrylaldehyde (**M1**, 0.87 wt%), 4-ethyl-2,6-dimethoxy-3-methylphenol (**M2**, 0.2 wt%), and 4-ethyl-2,6-dimethoxyphenol (**M3**, 0.1 wt%).[93] The formation of these products can be attributed to the cleavage of β-O-4 linkages within the oxidized lignin structure. Consistently, heteronuclear single quantum coherence (HSQC) spectroscopy of the insoluble solid fraction showed the disappearance of characteristic signals corresponding to β-O-4 linkages, further confirming their cleavage during the depolymerization process.[93]

On the other hand, $\mathbf{ITSO_2}$ was attempted for the upcycling of polystyrene (PS) due to its strongly oxidizing capacity (Fig. 4A). Unlike previous studies using HAT photocatalysts to abstract hydrogen atoms from the benzylic position for the subsequent cleavage of PS,[63] photocatalysis with $\mathbf{ITSO_2}$ may offer a complementary upcycling strategy by directly oxidizing non-activated arene groups. Initially, commercial PS, with a mass average molecular weight (M_w) of 560 966 g mol^{-1}, a number average molecular weight (M_n) of 198 240 g mol^{-1}, and a polydispersity index (PDI) of 2.83, was tested (left column, Fig. 4A). Irradiating PS in the presence of $\mathbf{ITSO_2}$ in 1,2-dichloroethane under an oxygen atmosphere using blue LEDs for 24 hours resulted in a transparent, clear solution, from which benzoic acid was isolated in 57% yield (entry 1). The gel permeation chromatography (GPC) analysis of the reaction mixture after photocatalytic upcycling confirmed the complete degradation of PS (Fig. S19 in the ESI†). Optimization of the reaction conditions revealed that solvents play a crucial role in this upcycling process. While dichloromethane, ethyl acetate, and acetone were effective solvents, no reaction occurred when acetonitrile, dimethyl sulfoxide, methanol, tetrahydrofuran, or toluene were used (entries 2–5). Control experiments confirmed that both the photocatalyst and visible light are essential (entries 6 and 7). This upcycling protocol is appealing due to its extremely mild reaction conditions, high selectivity for converting PS into benzoic acid, and the absence of any metals or acids.

To demonstrate the generality of the oxidative upcycling strategy, several plastics were investigated under the optimized reaction conditions (right column, Fig. 4A). General-purpose polystyrene (GPPS), a rigid and transparent polymer, was efficiently converted into benzoic acid with 56% yield under the photocatalysis of $\mathbf{ITSO_2}$. Expandable polystyrene (EPS), an elastic polymer containing azodicarbonamide as a foaming agent for enhanced impact resistance, underwent degradation to afford benzoic acid in 56% yield. High-impact polystyrene (HIPS), a graft copolymer composed of styrene and butadiene with notable impact strength, was successfully transformed into benzoic acid with 56% yield. Styrene–butadiene–acrylonitrile copolymers, including styrene–acrylonitrile (SAN) and acrylonitrile–butadiene–styrene (ABS), are widely utilized for their superior heat resistance and stability. Due to their chemical recalcitrance, the degradation of SAN and ABS did not occur under standard reaction conditions. However, when 4,5,6,7-tetrachloro-2-hydroxy-isoindole-1,3-dione (TCNHPI) was employed as an additive, SAN and ABS were effectively upcycled into benzoic acid in 54% yield and 48% yield, respectively. It was proposed that TCNHPI could serve as a hydrogen atom transfer agent to facilitate the degradation process (Tables S4, S5 and Fig. S33 in the ESI†).[93] Intriguingly, this protocol is applicable to the upcycling of mixed plastics. A mixture of PS, GPPS, EPS, HIPS, SAN, and ABS can be uniformly converted into benzoic acid in 50% yield under the photocatalysis of $\mathbf{ITSO_2}$ (Fig. 4A).

Next, PS waste from our daily life was investigated (Fig. 4B). Despite the presence of various additives in real-life plastics, this upcycling method demonstrated excellent compatibility with a wide range of plastic waste materials. As illustrated in Fig. 4B, all selected real-life plastics underwent smooth degradation into benzoic acid with high selectivity. Specifically, PS waste, including laboratory weighing boats, yogurt boxes, rulers, and plastic forks, was successfully converted into the desired benzoic acid under standard conditions (50–55% yields). Additionally, EPS waste, such as foam boxes and

shockproof foam, was effectively processed, producing benzoic acid in 57% yield and 56% yield, respectively. ABS waste from items like magic cubes, table tennis balls, plastic fans, and toy vehicles was also compatible with this protocol, delivering benzoic acid in 45–49% yields. Similarly, SAN waste from plastic cup was upcycled into benzoic acid in 46% yield.

The feasibility of **ITSO$_2$** photocatalysis for aerobic degradation of commercial PS, mixed PS, and PS waste from daily life has been demonstrated. To explore the scalability of this upcycling protocol, a continuous flow photoreactor was implemented (Fig. 4C). Using this flow technology, 1.04 g of commercial polystyrene was successfully converted into benzoic acid in 50% yield. More intriguingly, a gram-scale mixture of real-life plastics, including yogurt boxes, rulers, plastic forks, foam boxes, and shockproof foam, underwent upcycling to benzoic acid in 41% yield. These results clearly demonstrate the practicality and scalability of the **ITSO$_2$** photocatalysis protocol for the upcycling of plastic wastes.

To achieve the recyclability, the immobilization of **ITS** and **ITSO$_2$** on polymer supports has been explored. With the growing emphasis on the valorization of biomass derivatives and plastic waste, aforementioned studies have focused on converting oxidized lignin and polystyrene into value-added small molecules. As an alternative approach for repurposing these materials, we hypothesize that polystyrene and oxidized lignin can be employed as supports for the development of recyclable photocatalysts. To this end, **ITS** and **ITSO$_2$** were immobilized on polystyrene and oxidized lignin supports, respectively.[93] As depicted in Fig. 5A, **ITS@PS** was synthesized through the substitution reaction of **ITS**-derived carboxylic acid (**14**) with polymer (chloromethyl)polystyrene (**15**). Pleasingly, sequential photocatalytic cleavage of five varieties of oxidized β-O-4 lignin models was achieved using a single batch of **ITS@PS** added at the beginning of the reaction sequence, with comparable efficiency to that of homogeneous **ITS**. Notably, the heterogeneous photocatalyst can be easily separated from the reaction mixture *via* filtration and washing, then dried and reused directly without further purification.[93] Similarly, **ITSO$_2$@oxidized lignin** was prepared *via* the condensation reaction of **ITSO$_2$**-derived carboxylic acid (**16**) with primary alcohols present in oxidized lignin (**6**). The resultant **ITSO$_2$@-oxidized lignin** was found to catalyze the aerobic degradation of

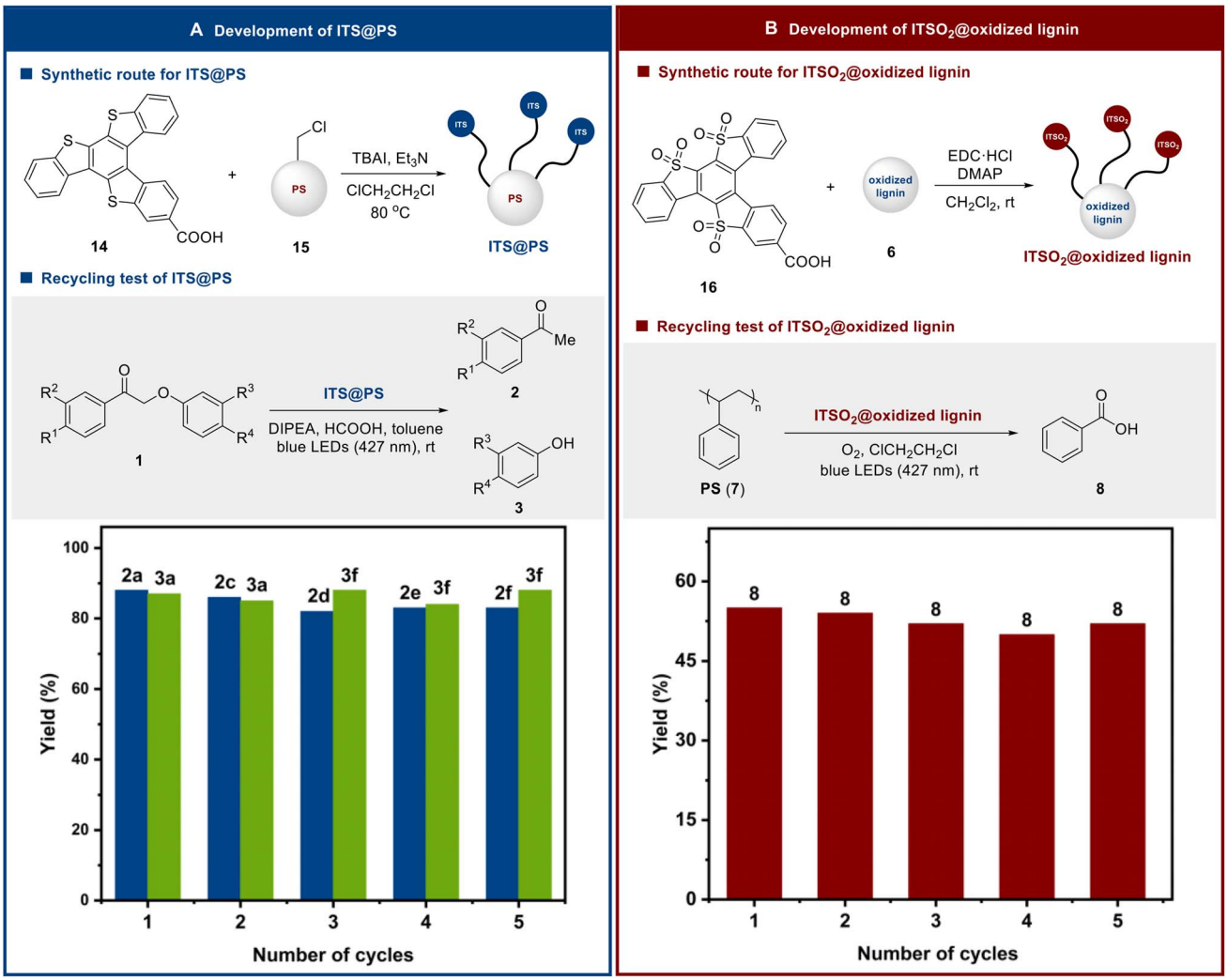

Fig. 5 Development of recyclable polymer-supported ITS and ITSO$_2$.

commercial PS for at least five cycles without an apparent decrease in the yields (Fig. 5B). Thus, **ITS@PS** and **$ITSO_2$@-oxidized lignin** represent a new class of recoverable and reusable photocatalysts that enable the upcycling of biomass derivatives and plastic wastes in a sustainable fashion.

To elucidate the mechanism, a series of Stern–Volmer quenching experiments were conducted based on each component involved in the cleavage of the oxidized β-O-4 lignin model **1a** (Fig. 6A). The results demonstrated that the excited state of **ITS** was significantly quenched by the ketone-containing substrate **1a**, whereas no significant quenching was observed with DIPEA or HCOOH. These findings support the hypothesis that the excited state of **ITS** (**ITS***) can directly facilitate SET reduction of ketone compounds, consistent with its favorable redox potential ($E^*_{1/2} = -2.17$ V). Regarding the photocatalytic upcycling of polystyrene, isopropylbenzene (**17**) was used as a model substrate to probe the mechanism. Stern–Volmer quenching experiments involving **17** confirmed that the excited state of $ITSO_2$ ($ITSO_2^*$)($E^*_{1/2} = +2.39$ V) can undergo SET oxidation of unactivated arenes. This is attributed to the strongly oxidizing capacity of $ITSO_2^*$, which contrasts with the mechanism of commonly used HAT photocatalysts.[63] Thus, **ITS** and $ITSO_2$ are highly reducing and oxidizing photocatalysts, respectively, capable of activating inert substrates directly. Besides, electron paramagnetic resonance (EPR) experiments were conducted using dimethylpyridine *N*-oxide (DMPO) or 2,2,6,6-tetramethylpiperidine (TEMP) as the free radical spin-trapping reagent (Fig. S30 in the ESI†). Upon irradiation, characteristic signals with six lines were observed, which match well with the DMPO–carbon-centered radical adduct under **ITS** photocatalysis. Meanwhile, the typical signals of DMPO–$O_2^{\bullet-}$ and TEMP–$^1O_2$ were both detected, indicating the generation of superoxide radical and singlet oxygen species under $ITSO_2$ photocatalysis.[93]

As illustrated in Fig. 6B, plausible mechanism is proposed using the cleavage of oxidized β-O-4 lignin model **1a** and the upcycling of polystyrene as the illustrative examples.[93] Upon irradiation, **ITS** reaches its excited state (**ITS***). Oxidative quenching of **ITS*** by **1a** generates $ITS^{\bullet+}$ and the corresponding ketyl radical (**I**), which fragments to yield the α-carbonyl radical **II** and 4-biphenylol (**3a**) after protonation. Subsequently, DIPEA donates an electron to convert $ITS^{\bullet+}$ back to **ITS**, thereby completing the photocatalytic cycle of **ITS**. Meanwhile, *p*-methoxyacetophenone (**2a**) is obtained by accepting both

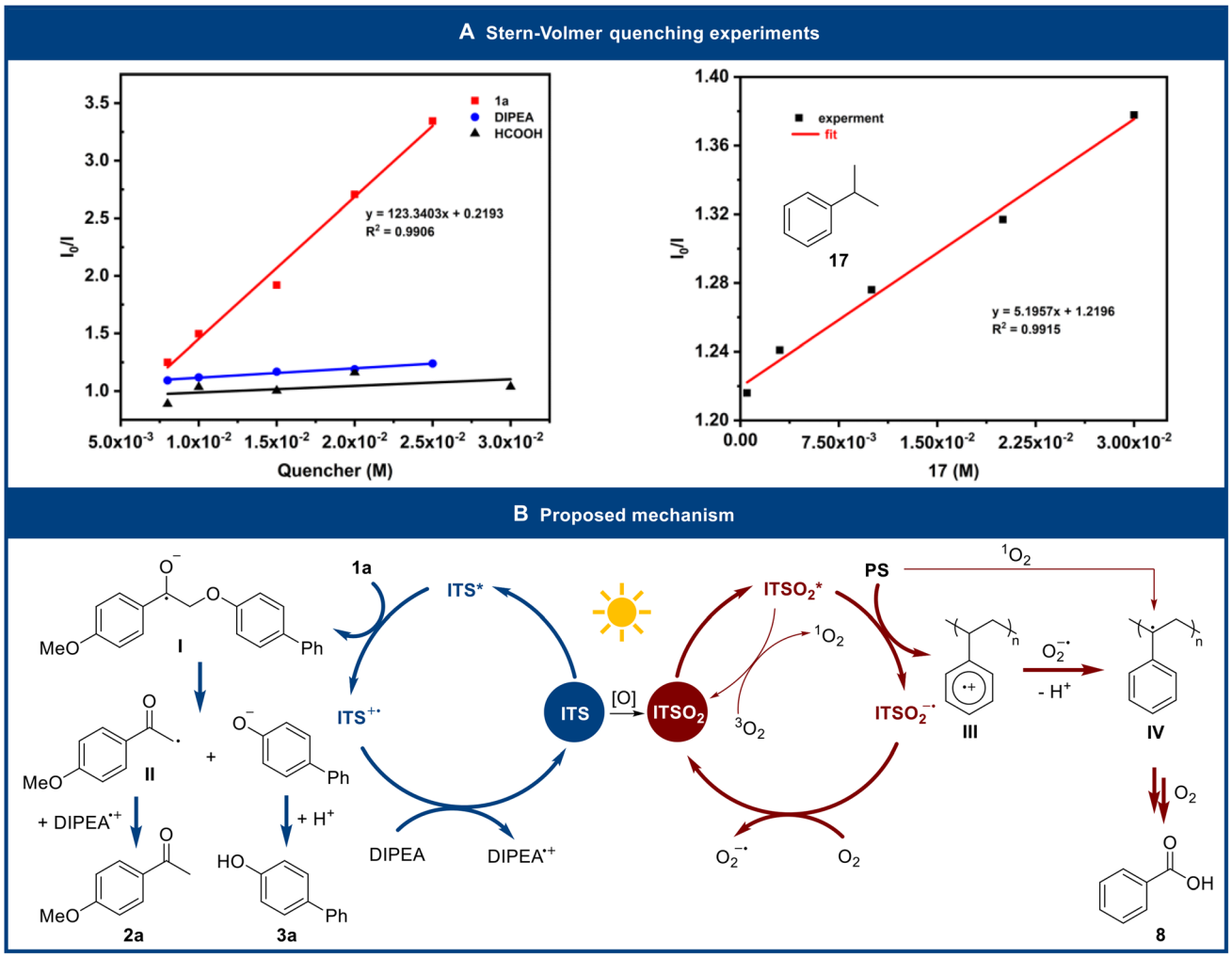

Fig. 6 Mechanistic studies.

electron and proton from DIPEA$^{\bullet+}$. On the other hand, $\mathbf{ITSO_2^*}$ undergoes SET oxidation of PS, affording the radical cation intermediate **III** and $\mathbf{ITSO_2}^{\bullet-}$. $\mathbf{ITSO_2}^{\bullet-}$ is regenerated to $\mathbf{ITSO_2}$ through oxidation by O_2, thus closing the photocatalytic cycle of $\mathbf{ITSO_2}$. The resultant superoxide radical anion $O_2^{\bullet-}$ abstracts a proton from intermediate **III** to form a benzylic radical intermediate **IV**, which then reacts with oxygen to induce the upcycling process, ultimately yielding benzoic acid (**8**). Alternatively, the degradation can proceed *via* an energy transfer mechanism involving singlet oxygen as the key intermediate.[74]

Conclusions

In summary, we have developed a pair of photocatalysts, isothiatruxene (**ITS**) and isosulfonyltruxene ($\mathbf{ITSO_2}$), through precise modulation of the valence states of heteroatoms. These photocatalysts are distinguished by their metal-free nature, cost-effectiveness, and facile synthesis *via* trimerization. More importantly, **ITS** and $\mathbf{ITSO_2}$ exhibit both strongly reducing and oxidizing capacities, with a combined redox potential window that exceeds those of conventional photocatalysts. Under **ITS** catalysis, photocatalytic reductive cleavage of C–O bonds in oxidized lignin models, vanillin-derived crosslinked polymer, and native oxidized lignin is achieved at room temperature. Conversely, $\mathbf{ITSO_2}$ catalysis enables photocatalytic oxidative upcycling of polystyrene and real-life plastics to benzoic acid in a metal-free and acid-free fashion. The implementation of flow technology allows for gram-scale upcycling of polystyrene. In addition, the recyclability of these photocatalysts is accomplished by immobilizing **ITS** and $\mathbf{ITSO_2}$ on polystyrene and oxidized lignin supports, respectively. Consistent with their strong redox capacities, mechanistic investigations confirm that the excited states of **ITS** and $\mathbf{ITSO_2}$ can directly activate biomass derivatives and plastic wastes, despite the demanding redox potentials. This study not only presents a novel strategy to access two significant opposing redox properties by tuning the valence states of heteroatoms, but also demonstrates a sustainable catalytic approach for the synthesis of value-added aromatic compounds from biomass derivatives and real-life plastic wastes. It is anticipated that this pair of photocatalysts may lead to the discovery of new challenging transformations.

Data availability

The data supporting this article have been included as part of the ESI.†

Author contributions

X. Z. conceived the project. H. C., X. C., X. S., W.-X. S., and S.-C. C. performed the experiments. H. C., X. C., and X. Z. cowrote the paper.

Conflicts of interest

A patent has been filed on this work.

Acknowledgements

We thank the National Natural Science Foundation of China (grant no. 22071024 and 22271047), and the Natural Science Foundation of Fujian Province (grant no. 2024J01290) for generous financial support. We also thank Prof. Chenguang Liu (Fuzhou University) for the assistance with flow photoreactor. The image of a tree in the graphical abstract and Fig. 1 is reproduced from H. Jiang, M. Liu, X. Lian, M. Zhu and F. Zhang, *Angew. Chem., Int. Ed.*, 2024, **63**, e202318850, DOI: **10.1002/anie.202318850**, with permission.

Notes and references

1 C. K. Prier, D. A. Rankic and D. W. C. Macmillan, *Chem. Rev.*, 2013, **113**, 5322.
2 N. A. Romero and D. A. Nicewicz, *Chem. Rev.*, 2016, **116**, 10075.
3 Q. Liu and L.-Z. Wu, *Natl. Sci. Rev.*, 2017, **4**, 359.
4 Y. Chen, L.-Q. Lu, D.-G. Yu, C.-J. Zhu and W.-J. Xiao, *Sci. China Chem.*, 2019, **62**, 24.
5 A. Vega-Peñaloza, J. Mateos, X. Companyó, M. Escudero-Casao and L. Dell'Amico, *Angew. Chem., Int. Ed.*, 2021, **60**, 1082.
6 A. Tlili and S. Lakhdar, *Angew. Chem., Int. Ed.*, 2021, **60**, 19526.
7 J. D. Bell and J. A. Murphy, *Chem. Soc. Rev.*, 2021, **50**, 9540.
8 T. Bortolato, S. Cuadros, G. Simionato and L. Dell'amico, *Chem. Commun.*, 2022, **58**, 1263.
9 C. Zhou, B. An, F. Lan and X. Zhang, *Chem. Commun.*, 2023, **59**, 13245.
10 L.-W. Wu, H. Cui and X. Zhang, *Chin. J. Org. Chem.*, 2025, **45**, 1097.
11 T. Huang, P. Du, X. Cheng and Y.-M. Lin, *J. Am. Chem. Soc.*, 2024, **146**, 24515.
12 M. Schmalzbauer, M. Marcon and B. König, *Angew. Chem., Int. Ed.*, 2021, **60**, 6270.
13 L.-L. Liao, L. Song, S.-S. Yan, J.-H. Ye and D.-G. Yu, *Trends Chem.*, 2022, **4**, 512.
14 I. A. Mackenzie, L. Wang, N. P. R. Onuska, O. F. Williams, K. Begam, A. M. Moran, B. D. Dunietz and D. A. Nicewicz, *Nature*, 2020, **580**, 76.
15 K. Liang, Q. Liu, L. Shen, X. Li, D. Wei, L. Zheng and C. Xia, *Chem. Sci.*, 2020, **11**, 6996.
16 Y. Li, Z. Ye, Y.-M. Lin, Y. Liu, Y. Zhang and L. Gong, *Nat. Commun.*, 2021, **12**, 2894.
17 S. Wang, H. Wang and B. König, *Chem*, 2021, **7**, 1653.
18 H. Li, X. Tang, J. H. Pang, X. Wu, E. K. L. Yeow, J. Wu and S. Chiba, *J. Am. Chem. Soc.*, 2021, **143**, 481.
19 J. Xu, J. Cao, X. Wu, H. Wang, X. Yang, X. Tang, R. W. Toh, R. Zhou, E. K. L. Yeow and J. Wu, *J. Am. Chem. Soc.*, 2021, **143**, 13266.
20 Q. Ma, J. Song, X. Zhang, Y. Jiang, L. Ji and S. Liao, *Nat. Commun.*, 2021, **12**, 429.
21 H. Li and O. S. Wenger, *Angew. Chem., Int. Ed.*, 2022, **61**, e202110491.

22 Y. Kwon, J. Lee, Y. Noh, D. Kim, Y. Lee, C. Yu, J. C. Roldao, S. Feng, J. Gierschner, R. Wannemacher and M. S. Kwon, *Nat. Commun.*, 2023, **14**, 92.
23 D. M. Fischer, H. Lindner, W. M. Amberg and E. M. Carreira, *J. Am. Chem. Soc.*, 2023, **145**, 774.
24 T. Bortolato, G. Simionato, M. Vayer, C. Rosso, L. Paoloni, E. M. Benetti, A. Sartorel, D. Lebœuf and L. Dell'Amico, *J. Am. Chem. Soc.*, 2023, **145**, 1835.
25 Y. Baek, A. Reinhold, L. Tian, P. D. Jeffrey, G. D. Scholes and R. R. Knowles, *J. Am. Chem. Soc.*, 2023, **145**, 12499.
26 S. Halder, S. Mandal, A. Kundu, B. Mandal and D. Adhikari, *J. Am. Chem. Soc.*, 2023, **145**, 22403.
27 B. Pfund, V. Hutskalova, C. Sparr and O. S. Wenger, *Chem. Sci.*, 2023, **14**, 11180.
28 K. Liang, X. Li, D. Wei, C. Jin, C. Liu and C. Xia, *Chem*, 2023, **9**, 511.
29 L. Bai and L. Jiao, *Chem*, 2023, **9**, 3245.
30 B. An, H. Cui, C. Zheng, J.-L. Chen, F. Lan, S.-L. You and X. Zhang, *Chem. Sci.*, 2024, **15**, 4114.
31 C. Liu, Y. Zhang and R. Shang, *Chem*, 2025, **11**, 102359.
32 S. Okumura, S. Hattori, L. Fang and Y. Uozumi, *J. Am. Chem. Soc.*, 2024, **146**, 16990.
33 H. Zhang, J.-X. Chen, J.-P. Qu and Y.-B. Kang, *Nature*, 2024, **635**, 610.
34 X. Liu, A. Sau, A. R. Green, M. V. Popescu, N. F. Pompetti, Y. Li, Y. Zhao, R. S. Paton, N. H. Damrauer and G. M. Miyake, *Nature*, 2025, **637**, 601.
35 S. Fukuzumi, H. Kotani, K. Ohkubo, S. Ogo, N. V. Tkachenko and H. Lemmetyinen, *J. Am. Chem. Soc.*, 2004, **126**, 1600.
36 H. Cheng, X. Wang, L. Chang, Y. Chen, L. Chu and Z. Zuo, *Sci. Bull.*, 2019, **64**, 1896.
37 H. Yan, J. Song, S. Zhu and H.-C. Xu, *CCS Chem.*, 2021, **3**, 317.
38 H. Huang, Y. Jiang, W. Yuan and Y.-M. Lin, *Angew. Chem., Int. Ed.*, 2024, **63**, e202409653.
39 S. C. Sau, M. Schmitz, C. Burdenski, M. Baumert, P. W. Antoni, C. Kerzig and M. M. Hansmann, *J. Am. Chem. Soc.*, 2024, **146**, 3416.
40 M. R. Lasky, E.-C. Liu, M. S. Remy and M. S. Sanford, *J. Am. Chem. Soc.*, 2024, **146**, 14799.
41 C.-H. Hu, Y. Sang, Y.-W. Yang, W.-W. Li, H.-L. Wang, Z. Y. Zhang, C. Ye, L.-Z. Wu, X.-S. Xue and Y. Li, *Chem*, 2023, **9**, 2997.
42 A. Singh, K. Teegardin, M. Kelly, K. S. Prasad, S. Krishnan and J. D. Weaver, *J. Organomet. Chem.*, 2015, **776**, 51.
43 E. Speckmeier, T. G. Fischer and K. Zeitler, *J. Am. Chem. Soc.*, 2018, **140**, 15353.
44 C. Xu, R. A. D. Arancon, J. Labidi and R. Luque, *Chem. Soc. Rev.*, 2014, **43**, 7485.
45 S. S. Wong, R. Shu, J. Zhang, H. Liu and N. Yan, *Chem. Soc. Rev.*, 2020, **49**, 5510.
46 C. Zhang and F. Wang, *Acc. Chem. Res.*, 2020, **53**, 470.
47 K. Lee, Y. Jing, Y. Wang and N. Yan, *Nat. Rev. Chem.*, 2022, **6**, 635.
48 D. Aboagye, R. Djellabi, F. Medina and S. Contreras, *Angew. Chem., Int. Ed.*, 2023, **62**, e202301909.
49 S. Zheng, Z. Zhang, S. He, H. Yang, H. Atia, A. M. Abdel-Mageed, S. Wohlrab, E. Baráth, S. Tin, H. J. Heeres, P. J. Deuss and J. G. de Vries, *Chem. Rev.*, 2024, **124**, 10701.
50 M. Macleod, H. P. H. Arp, M. B. Tekman and A. Jahnke, *Science*, 2021, **373**, 61.
51 L. T. J. Korley, T. H. Epps, B. A. Helms and A. J. Ryan, *Science*, 2021, **373**, 66.
52 L. D. Ellis, N. A. Rorrer, K. P. Sullivan, M. Otto, J. E. McGeehan, Y. Román-Leshkov, N. Wierckx and G. T. Beckham, *Nat. Catal.*, 2021, **4**, 539.
53 C. Jehanno, J. W. Alty, M. Roosen, S. D. Meester, A. P. Dove, E. Y.-X. Chen, F. A. Leibfarth and H. Sardon, *Nature*, 2022, **603**, 803.
54 M.-Q. Zhang, M. Wang, B. Sun, C. Hu, D. Xiao and D. Ma, *Chem*, 2022, **8**, 2912.
55 E. Skolia, O. G. Mountanea and C. G. Kokotos, *Trends Chem.*, 2023, **5**, 116.
56 F. Eisenreich, *Angew. Chem., Int. Ed.*, 2023, **62**, e202301303.
57 O. Guselnikova, O. Semyonov, E. Sviridova, R. Gulyaev, A. Gorbunova, D. Kogolev, A. Trelin, Y. Yamauchi, R. Boukherroub and P. Postnikov, *Chem. Soc. Rev.*, 2023, **52**, 4755.
58 B. Qin and X. Zhang, *CCS Chem.*, 2024, **6**, 297.
59 L. Gan, Z. Dong, H. Xu, H. Lv, G. Liu, F. Zhang and Z. Huang, *CCS Chem.*, 2024, **6**, 313.
60 K. Su, T. Gao, C.-H. Tung and L.-Z. Wu, *Angew. Chem., Int. Ed.*, 2024, **63**, e202407464.
61 S. Feng, P. T. T. Nguyen, X. Ma and N. Yan, *Angew. Chem., Int. Ed.*, 2024, **63**, e202408504.
62 S. Oh and E. E. Stache, *Chem. Soc. Rev.*, 2024, **53**, 7309.
63 H. Cui, X. Chen, F. Lan, B. An and X. Zhang, *Trends Chem.*, 2024, **6**, 392.
64 D. Sajwan, A. Sharma, M. Sharma and V. Krishnan, *ACS Catal.*, 2024, **14**, 4865.
65 S. Jiang, Y. Chen, Y. Huang and P. Hu, *Eur. J. Org Chem.*, 2025, **28**, e202401109.
66 E. Skolia, O. G. Mountanea and C. G. Kokotos, *ChemSusChem*, 2024, **17**, e202400174.
67 Z. Xu, D. Sun, J. Xu, R. Yang, J. D. Russell and G. Liu, *ChemSusChem*, 2024, **17**, e202400474.
68 H. Jiang, M. Liu, X. Lian, M. Zhu and F. Zhang, *Angew. Chem., Int. Ed.*, 2024, **63**, e202318850.
69 M. Wang, J. Wen, Y. Huang and P. Hu, *ChemSusChem*, 2021, **14**, 5049.
70 J. D. Nguyen, B. S. Matsuura and C. R. J. Stephenson, *J. Am. Chem. Soc.*, 2014, **136**, 1218.
71 H. Guo, D. M. Miles-Barrett, A. R. Neal, T. Zhang, C. Li and N. J. Westwood, *Chem. Sci.*, 2018, **9**, 702.
72 G. Zhang, Z. Zhang and R. Zeng, *Chin. J. Chem.*, 2021, **39**, 3225.
73 S. Oh and E. E. Stache, *J. Am. Chem. Soc.*, 2022, **144**, 5745.
74 Z. Huang, M. Shanmugam, Z. Liu, A. Brookfield, E. L. Bennett, R. Guan, D. E. V. Herrera, J. A. Lopez-Sanchez, A. G. Slater, E. J. L. Mclnnes, X. Qi and J. Xiao, *J. Am. Chem. Soc.*, 2022, **144**, 6532.
75 Y. Qin, T. Zhang, H. Y. V. Ching, G. S. Raman and S. Das, *Chem*, 2022, **8**, 2472.

76 R. Cao, M.-Q. Zhang, C. Hu, D. Xiao, M. Wang and D. Ma, *Nat. Commun.*, 2022, **13**, 4809.
77 T. Li, A. Vijeta, C. Casadevall, A. S. Gentleman, T. Euser and E. Reisner, *ACS Catal.*, 2022, **12**, 8155.
78 J. Meng, Y. Zhou, D. Li and X. Jiang, *Sci. Bull.*, 2023, **68**, 1522.
79 C. Li, X. Y. Kong, M. Lyu, X. T. Tay, M. Đokić, K. F. Chin, C. T. Yang, E. K. X. Lee, J. Zhang, C. Y. Tham, W. X. Chan, W. J. Lee, T. T. Lim, A. Goto, M. B. Sullivan and H. S. Soo, *Chem*, 2023, **9**, 2683.
80 N. F. Nikitas, E. Skolia, P. L. Gkizis, I. Triandafillidi and C. G. Kokotos, *Green Chem.*, 2023, **25**, 4750.
81 A. Ong, Z. C. Wong, K. L. O. Chin, W. W. Loh, M. H. Chua, S. J. Ang and J. Y. C. Lim, *Chem. Sci.*, 2024, **15**, 1061.
82 B. Zhao, H. Tan, J. Yang, X. Zhang, Z. Yu, H. Sun, J. Wei, X. Zhao, Y. Zhang, L. Chen, D. Yang, J. Deng, Y. Fu, Z. Huang and N. Jiao, *Innovation*, 2024, **5**, 100586.
83 W. X. Chan, X. Y. Kong, S. R. Choo and H. S. Soo, *Chem Catal.*, 2024, **4**, 101044.
84 L. Wimberger, G. Ng and C. Boyer, *Nat. Commun.*, 2024, **15**, 2510.
85 S.-Q. Chen, Q.-S. Huang, Y. Li, J. Wu, S. Chen and Z.-F. Yan, *J. Hazard. Mater.*, 2024, **480**, 135895.
86 D. Shao, W. Zhao, S. Ji, C. Yang, J. Zhang, R. Guo, B. Zhang, W. Lyu, J. Feng, H. Xu, W. Yan and H. Song, *Appl. Catal. B Environ.*, 2024, **357**, 124281.
87 A.-L. De Abreu, D. Taton and D. M. Bassani, *Angew. Chem., Int. Ed.*, 2025, **64**, e202418680.
88 E. Xu, T. Liu, F. Xie, J. He and Y. Zhang, *Chem. Sci.*, 2025, **16**, 2004.
89 C. E. Dalgliesh and F. G. Mann, *J. Chem. Soc.*, 1945, 910.
90 H. Y. Cho and L. T. Scott, *Tetrahedron Lett.*, 2015, **56**, 3458.
91 C. Zhou, X. Zhao and X. Zhang, *Chin. J. Org. Chem.*, 2025, **45**, 42.
92 H. G. Roth, N. A. Romero and D. A. Nicewicz, *Synlett*, 2016, **27**, 714.
93 See the ESI† for more details.
94 R. Singathi, R. Raghunathan, R. Krishnan, S. K. Rajendran, S. Baburaj, M. P. Sibi, D. C. Webster and J. Sivaguru, *Angew. Chem., Int. Ed.*, 2022, **61**, e202203353.